Flammability of EVA/IFR (APP/PER/ZB System) and EVA/IFR/Synergist ($CaCO_3$, NG, and EG) Composites

Xinfeng Wu, Lichun Wang, Chao Wu, Genlin Wang, Pingkai Jiang

Shanghai Key Laboratory of Electrical Insulation and Thermal Aging, Department of Polymer Science and Engineering, Shanghai Jiao Tong University, Shanghai 200240, China

Received 18 July 2011; accepted 27 January 2012
DOI 10.1002/app.36884
Published online in Wiley Online Library (wileyonlinelibrary.com).

ABSTRACT: Poly(ethylene-*co*-vinyl acetate)/intumescent flame retardant (ammonium polyphosphate/pentaerythritol/zinc borate system) composites-EVA/IFR (APP/PER/ZB system) and EVA/IFR/Synergist [$CaCO_3$, natural graphite, or expanded graphite (EG)] composites have been prepared by melting compounding method. The flammability, the combustion process, the quantity of the residual chars, the morphology of the residual chars, and the thermal stability of the chars have been investigated by cone calorimeter, scanning electron microscopy and thermo gravimetric analysis. The results indicate that heat release rate (HRR), total heat released, and total smoke release (TSR) of EVA/IFR (IFR 30 phr) composite decrease to about 67.1, 78.2, and 64% of that of pure EVA, respectively. HRR, THR, and TSR of EVA/IFR/EG (IFR 9 phr, EG 1phr) composite decrease to about 62.1, 76.2, and 44% of that of pure EVA, respectively. The quantity, the thermal stability of residual chars and the char structure are discussed to find the reasons of the phenomenon above. It has been found that the flame retardant of EVA vulcanizates is improved and the fire jeopardizing is dramatically reduced due to the addition of IFR and synergist, which can give some advice to design formulations for practical applications as cable. © 2012 Wiley Periodicals, Inc. J Appl Polym Sci 000: 000–000, 2012

Key words: EVA; APP/PER/ZB; intumescent flame retardant; synergist

INTRODUCTION

EVA is suitable for use in the wire and cable industry as insulating materials due to its good mechanical and physical properties.[1–5] The polymer is easily flammable due to its chemical constitution, so the flame retardancy becomes an important requirement for the industry.[6–17] This problem could be solved by using flame retardant additives, such as halogenated compounds with antimony trioxide.[18] However, their fire retardant action may be accompanied by negative effects such as generation of corrosive, obscuring, and toxic smoke.[19,20] To improve the protection of human health and the environment through the better and earlier identification of the intrinsic properties of chemical substances, the new regulations like the European Directives on WEEE, RoHS, and REACH restrict the demand for some brominated flame retardants (such as polybrominated biphenyl, polybrominated diphenyl ethers, and hexabromocyclododecane). Therefore, it is worthwhile to investigate the halogen-free flame retardation of the polymer. The compounds used as halogen-free flame-retardants in EVA include metal hydroxides, phosphorous, or phosphorous/nitrogen-containing compounds, etc. Metal hydroxides, mainly magnesium hydroxide and aluminum hydroxide, are commonly used in the flame retardation of polymers due to their no toxicity and moderate cost.[21–24] However, the high loadings required (>60 wt %) for adequate flame retardant level often lead to difficult processing and a great decrease in the mechanical properties of filled polymer materials.

In recent years, intumescent flame retardant (IFR) additives have been investigated by many researchers, and presenting good flame retardancy and excellent char forming ability in many polymeric materials. Generally, IFR include: (1) inorganic acid or precursors, such as phosphorous-containing compounds; (2) a carbon-rich polyhydric compound, such as pentaerythritol (PER); and (3) a blowing agent, such as melamine (MEL) and polyamides, to yield gaseous products. During combustion, the intumescent system forms an expanding charred crust as a barrier between the flame and the underlying polymeric material. This "c" compact rust attenuates the transfer of heat, limits the diffusion of oxygen and degraded products of the material.

The IFR technique has emerged as a promising method for conferring flame retardancy upon

Correspondence to: G. Wang (wanggenlin@sjtu.edu.cn) or P. Jiang (pkjiang@sjtu.edu.cn).

polymers, its merits including very low smoke and toxic gas production during burning, and an anti-dripping property. However, traditional IFRs (e. g., APP/PER/MEL system) have some drawbacks compared with bromine-containing flame retardants,[25,26] such as low flame-retardant efficiency, low thermal stability. These problems have seriously restricted IFR's applications in polymeric materials. To solve these drawbacks[27,28] mentioned above, a lot of synergistic additives as well as the combination of different fillers have been investigated to enhance the flame retardancy of IFR systems, such as organoclays or nanoclays,[3,29–34] some transitional metal oxides and metal compounds[35–39] [MoO_3, Fe_2O_3, TiO_2, La_2O_3, nickel formate, zinc borate (ZB), zirconium phosphate, and polyhedral oligomeric silsesquioxane],[40] natural or organo-modified silicates,[41–43] carbon nanotubes,[34,44–47] and some other synergistic agents (layered double hydroxides, zeolites, etc.).[48–54]

These relatively new materials containing a low amount of filler (<5 wt %) are able to slow down the combustion kinetics of EVA with a low emission of toxic smokes. It has been shown that synergists can effectively promote and catalyze a series of reactions including esterification, dehydration, and crosslinking among IFR components to improve the mechanical strengths and heat stabilities of char residues.[55,56] Synergistic flame retardant effects of IFR and filler are widely believed to be effective in reducing flammability and improving thermal stability for polyolefins.

In this work, IFR (APP/PER/ZB system) was used in EVA composites and $CaCO_3$, NG, and EG were used as charring synergistic agents for optimizing the flame retardancy of EVA/IFR composites. Their flammability performance and their properties of char (yield and thermal stability) were investigated by cone calorimeter, thermogravimetric analysis (TGA), respectively. The synergism between $CaCO_3$ or NG or EG and IFR in EVA matrix was studied; the morphology of the intumescent char layer and its possible mechanism were investigated by SEM.

The aim of this study was to evaluate the potential flame retardancy action of EVA/IFR composites and synergistic flame retardancy action of filler microparticles, more specifically $CaCO_3$, NG, and EG, when used in combination with IFR in EVA. The long-term goal of this work were, however, to probe the roles of microfillers playing in the intumescent flame retarded EVA composites; however, to determine optimal formulations that will be effective with respect to other multiple fire retardants, hence providing theoretical guidance to scientific research and industry.

EXPERIMENTS

Materials

A commercial cable grade EVA rubber (Levapren 500HV) was kindly supplied by Lanxess, Germany. The vinyl acetate content was 50 wt %, the Mooney viscosity was ML1 + 4 (100°C) = 27 ± 4, the MFI (ASTM D-1238, 100°C, and 1.2 kg) ≤5 g/min, and the density was 1.00 g/cm^3.

Dicumyl peroxide (DCP) used as a crosslinking agent was 99.3% pure and obtained from Shanghai Gaoqiao Petroleum, China. Crosslinking coagent triallyl isocyanurate (TAIC) and antioxidant dialkylated diphenylamine (DDA) were all supplied by Taizhou Huangyan Donghai chemical, China. NG (particle size: 300 μm) and expanded graphite (EG, particle size: 300 μm; Inflation rate: 300) were all acquired from Qingdao Xinghe Shimo, China. $CaCO_3$ (particle size: 5 μm), Shanghai Yihuan Chemical Industry, China. Ammonium Polyphosphate (APP, $(NH4PO_3)n$, $n > 50$, particle size: 10 μm), Shanghai Xusen Non-Halogen Smoke Suppressing Fire Retardants, China. Zinc stearate ($ZnSt_2$; particle size: 45 μm), PER (particle size: 45 μm), Shanghai Chemical reagent, China. ZB (particle size: 45 μm), Zibo Xubei Chemical, China.

Measurement and characterization

Cone calorimeter test

Cone calorimeter uses a truncated conical heater element to irradiate test specimens at heat fluxes from 10 to 100 kW/m^2, thereby simulating a range of fire intensities. The technique is a small scale fire test, but it has been shown to provide data that correlate well with those from full-scale fire tests. Cone calorimeter tests were carried out in duplicate, using a 35 kW/m^2 incident heat flux, following the procedures indicated in the ISO 5660 standard with a FTT cone calorimeter. Each specimen, of dimensions 10 × 10 × 0.3 cm^3, was wrapped in aluminum foil and placed on a mineral fiber blanket with the surface level with the holder, such that only the upper face was exposed to the radiant heater. The edge guard was used with all specimens, as was the recommended standard retaining grid to prevent excessive intumescence. The experimental error rate from the cone calorimeter test was about ± 5%. The cone calorimeter technique provides detailed information about ignition behavior, heat release, and smoke evolution during sustained combustion and some key parameters, which are correlated well with real fire.[57,58]

Thermogravimetric analysis

The TGA data were obtained in air at a heating rate of 20°C/min by a Perkin–Elmer Q 50 thermo

TABLE I
Formulations of EVA/IFR and Its Optimized Composites with $CaCO_3$, NG, and EG

Sample name	EVA (phr)	IFR (phr)	$CaCO_3$ (phr)	NG (phr)	EG (phr)	DCP (phr)	TAIC (phr)	DDA (phr)	$ZnSt_2$ (phr)
IFR 0	100	0	0	0	0	2.0	0.5	0.5	0.5
IFR 10	100	10	0	0	0	2.0	0.5	0.5	0.5
IFR 9/$CaCO_3$ 1	100	9	1	0	0	2.0	0.5	0.5	0.5
IFR 9/NG 1	100	9	0	1	0	2.0	0.5	0.5	0.5
IFR 9/EG 1	100	9	0	0	1	2.0	0.5	0.5	0.5
IFR 20	100	20	0	0	0	2.0	0.5	0.5	0.5
IFR 30	100	30	0	0	0	2.0	0.5	0.5	0.5

In IFR (APP/PER/ZB system), APP : PER : ZB = 3 : 1 : 1.

gravimetric analyzer. In each case, a 5–10 mg sample was examined under the gas (air) flow rate of 5×10^{-5} m^3/min at the temperatures ranging from room temperature to 800°C to evaluate the thermal stabilities of char residues left from Cone calorimeter test.

Microstructure analyses by SEM

SEM analyses for the morphology of residues of combustion by cone calorimeter were made using a field emission scanning electron microscopy (FE-SEM, JEOL JEM-4701). The gold-coated samples to avoid accumulation of charges were analyzed at an accelerating voltage of 20 kV.

Preparation of samples and crosslinking

EVA chemically crosslinked formulations (Table I), containing different loading (0–30 phr, parts per hundred of resin) of IFR as flame retardant and quantitative loading (1 phr) of $CaCO_3$, NG, or EG as synergist, were prepared through the following several steps. First, all additives except DCP were mixed with EVA for 8 min at 150°C with an internal mixer (XSS-300 Torque Rheometer, the chamber volume is 60 mL, Shanghai kechuang rubber, and plastic machinery equipment) at a speed of 50 rpm. Then, the mixture was moved into a two-roll mill, and DCP was added at 110°C and mixed for 3–5 min. Finally, crosslinking of the mixtures were performed and samples of EVA vulcanizates were prepared by using the molding of sheets at 180°C for 10 min.

RESULTS AND DISCUSSION

Flammability of EVA/IFR composites and EVA/IFR/synergist composites in cone calorimeter test

Cone calorimeter test based on the oxygen consumption principle has been widely used to evaluate the flammability performance of polymeric materials. Although cone calorimeter test is a small-scale test, the obtained results have been found to correlate well with those obtained from large-scale fire tests and can be used to predict the combustion behaviors of materials in a real fire.[59,60] By measuring the time to ignition (TTI), mass loss rate (MLR), total heat released (THR), and heat release rate (HRR), smoke production rate (SPR), and total smoke release (TSR), the flammability of the materials can be quantified.[61–63] Especially HRR, which is a very important parameter, can be used to express the intensity of a fire.[64] A highly flame retardant system normally shows a low HRR value. Table II shows the cone results of EVA/IFR and its optimized composites with $CaCO_3$, NG, and EG.

TABLE II
Cone Results of EVA/IFR and Its Optimized Composites with $CaCO_3$, NG, and EG

Sample name	TTI[a] (s)	PHRR[b] (kW/m^2)	AHRR[c] (kW/m^2)	THR (MJ/m^2)	FPI[d] ($m^2.s/kW$)	Residues (%)
IFR 0	53	836	315	101	0.063	1.5
IFR 10	44	745	302	98	0.059	6.8
IFR9/$CaCO_3$ 1	59	690	283	82	0.086	8.3
IFR 9/NG 1	58	568	274	80	0.102	8.6
IFR 9/EG 1	61	519	266	77	0.118	8.4
IFR 20	43	609	294	91	0.071	10.2
IFR 30	41	561	287	79	0.073	11.9

[a] Time to ignition.
[b] Peak of heat release rate, expressing the intensity of a fire.
[c] Average HRR within the front 200 s from heat radiation.
[d] Fire performance index, the ratio of TTI and PHRR.

Because of the close relationship between the ratio of TTI and PHRR (FPI) and the real fire condition, it is often the basis of escape time designing for firefighters in a real fire. The longer of the TTI and the lower of the PHRR, the higher of FPI and the better chance to reduce the loss and casualty in a real fire. From Table II, FPI of EVA/IFR composite increases to 0.073 from 0.059 with the increasing IFR content. Especially for EVA/IFR/EG composite, FPI increases to 0.118, about 1.78 times of pure EVA. The result that FPI of EVA/IFR (0.059, IFR 10) is lower than that of pure EVA may be explained that the contribution of IFR to TTI is lower than the contribution of IFR to PHRR. As a whole, the above results indicate that the flame retardant is improved for EVA vulcanizates by the addition of IFR and synergist, and which is very important for the practical usage as halogen-free flame retardants cable materials. The results of FPI provide the basis for estimation of both the predicted fire spread rate and the size of a fire[57] and is a good indicator of the contribution to fire growth of materials.

HRR of EVA/IFR composites and EVA/IFR/synergist composites

Figure 1 shows the dynamic curves of HRR versus time for various samples. From Figure 1(a) and Table II, it can be clearly seen that pure EVA burns very fast after ignition and a sharp HRR peak appears (at 150 s) with a peak heat release rate (PHRR) as high as 836 kW/m^2. With the addition of IFR, the flammability of the composites is obviously restrained, it could be found that the HRR and PHRR values reduce as the loading of IFR increases, and PHRR values of EVA/IFR samples (IFR 10–IFR 30) decrease to about 745, 609, and 561 kW/m^2, which are only 89.1, 72.8, and 67.1% of that of pure EVA (836 kW/m^2).

In Figure 1(b), we can see that PHRR ($CaCO_3$, NG, and EG as synergist, respectively) decreases to 690, 568, and 519 kW/m^2, respectively, which are 82.5, 67.9, and 62.1% of that of pure EVA and also all lower than that of IFR 10 specimen (745 kW/m^2), especially for PHRR of EVA/IFR/EG composite, which is even lower than that of IFR 30 specimen, showing the synergistic effect on EVA/IFR composites.

Because of the incomplete combustion of the composites, the average HRR (Av-HRR) of EVA /IFR (287 kW/m^2; IFR 30) and EVA/IFR/synergist (IFR 9/$CaCO_3$ 1, 283 kW/m^2; IFR 9/NG 1, 274 kW/m^2; IFR 9/EG 1, 266 kW/m^2) show a notable reduction with respect to that of pure EVA (315.0 kW/m^2).

In addition, it has been found that pure EVA only has a single HRR peak (Fig. 1). However, there are two peaks for some EVA/IFR and EVA/IFR/Synergist composites, which have good flame retardancy (a lower HRR). Bourbigot et al.[65] also found this phenomenon in exploring APP/MEL/PER intumescent systems, and also many other researches of IFRs.[57,66] The one HRR peak is easily understood because the sample is gradually burnt. In the second case, the first peak is assigned to the development of the intumescent protective char. After the first peak, the HRR curve forms a plateau in some cases, in which the increase in HRR is suppressed because of the presence of the efficient protective char. The second peak is due to the degradation of the protective layer gradually as the sample is continuously exposed to the heat and the formation of a new protective char in some formulations, which can be described in Figure 5.

From Figure 1(b), we can see that the second peaks of EVA/IFR/$CaCO_3$ and EVA/IFR/NG are not so obvious and the curves are not so smooth compared with EVA/IFR system, indicating that the protective char formed at the first stage is more stable than that of EVA/IFR system and not so easily

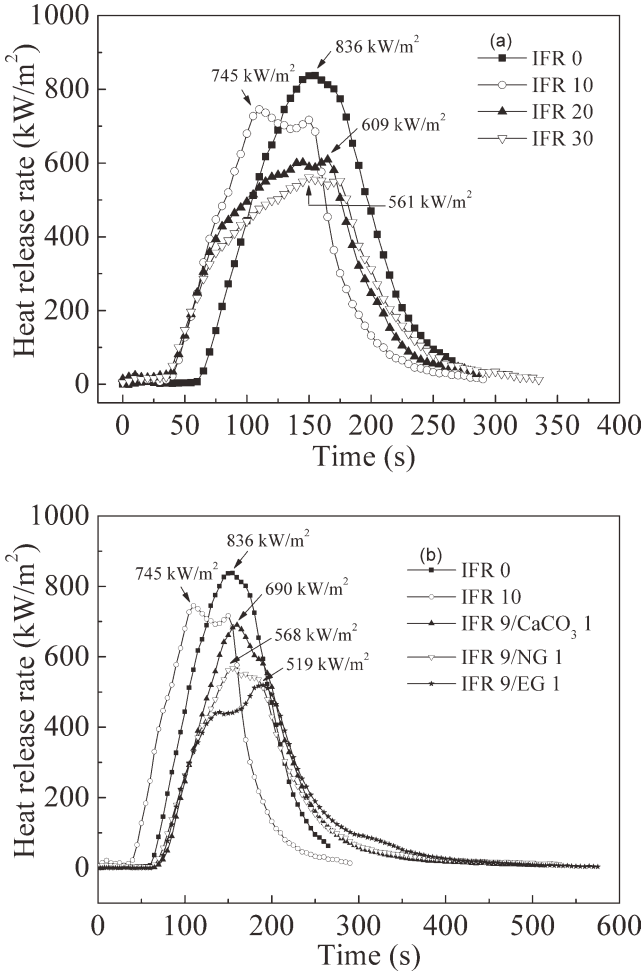

Figure 1 HRR curves versus time for EVA/IFR (APP/PER/ZB) (a) and its optimized composites with $CaCO_3$, NG and EG (b).

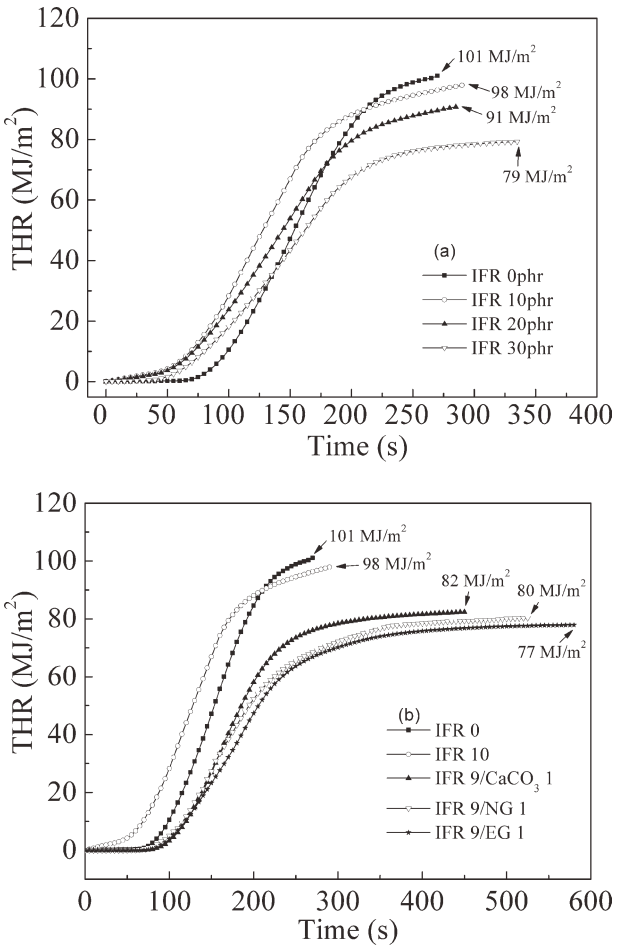

Figure 2 THR curves versus time for EVA/IFR (APP/PER/ZB) (a) and its optimized composites with $CaCO_3$, NG, and EG (b).

to be destroyed by the combustion. EG from NG, so it has some drawbacks that may not be resist the oxidation. The oxidation destroyed the char formed at the same stage, and then the more stable char formed quickly, explaining that the second peak of EVA/IFR/EG is higher than the first peak. Therefore, $CaCO_3$, NG, or EG addition can enhance the strength of char layer, prevent the char layer from cracking, enhance the char residue, and get a low HRR and THR. The enhancement of the strength of char layer can be in agreement with the TGA results discussed below.

THR of EVA/IFR composites and EVA/IFR/synergist composites

Figure 2 presents the THR curves of EVA and EVA/IFR with and without synergist composites, and the slope of THR curve is assumed as representative of fire spread rate.[67] Obviously, the flame spread rate as well as the THR energy of EVA/IFR (79 MJ/m^2; IFR 30) has decreased significantly compared to pure EVA (101 MJ/m^2), about 78.2% of that of pure EVA, indicating parts of the polymer are protected without completely combusted. The phenomenon can be explained that while burning, an intumescent char is formed on the surface of the matrix, which makes a thermal insulation and provokes the extinguishment of the flame and prevents combustible gases from feeding the flame, and separates oxygen from burning materials.[2]

THR of EVA/IFR/Synergist (82–77 MJ/m^2; about 81.2–76.2% of that of pure EVA) are lower than that of EVA/IFR (98 MJ/m^2; IFR 10), and the THR/total mass loss has the same tide with the average HRR. It means that the addition of synergist into the composite could induce the decrease of the heat generated. It knows that the HRR is a function of heat generation rate and heat transfer, and the heat generation rate is related with oxygen transfer during the combustion, so the decrease of HRR is mostly owing to the decrease of its transfer rate. In other words, the addition of synergist into the EVA/IFR composites could improve the barrier property of the char layer, and thus the transfer rate is retarded. In a word, the synergists have synergistic effect on the char formation of the composites.

SPR and TSR of EVA/IFR composites and EVA/IFR/synergist composites

Generally, the emission of smoke along with HRR also plays a critical role in fire conditions. The curves of SPR and TSR of EVA/IFR with and without synergist composites via time are seen in Figures 3 and 4. Similar to the HRR and THR curves, we can see that the SPR plots of EVA/IFR are lower than that of pure EVA and TSR of EVA/IFR decreases to 1600 m^2 (IFR 30) gradually from 2500 m^2 for pure EVA in Figure 3, about 64% of that of pure EVA, declaring that IFR has some effect of smoke suppression.

The SPR and TSR values for EVA/IFR/Synergist composites containing $CaCO_3$, NG, or EG are lower than that of EVA/IFR within 10 phr loading. TSR of EVA/IFR/EG is 1100 m^2, about 44% of that of pure EVA and is the lowest in the optimized formulation. The results meant that synergist perform an important function in smoke suppression and is better in smoke suppression than only using IFR. All the above changes indicate that the flame retardancy is improved further for the optimized EVA/IFR composites by addition of $CaCO_3$, NG, or EG.

From the results of the cone calorimeter test and analyses above, we can get a conclusion that the residual mass of the char and the strength of the residual char take a deterministic effect on the reduction of HRR, THR, SPR, and TSR. The residual mass of the char was tested by the cone calorimeter, the strength of the residual char was measured by TGA,

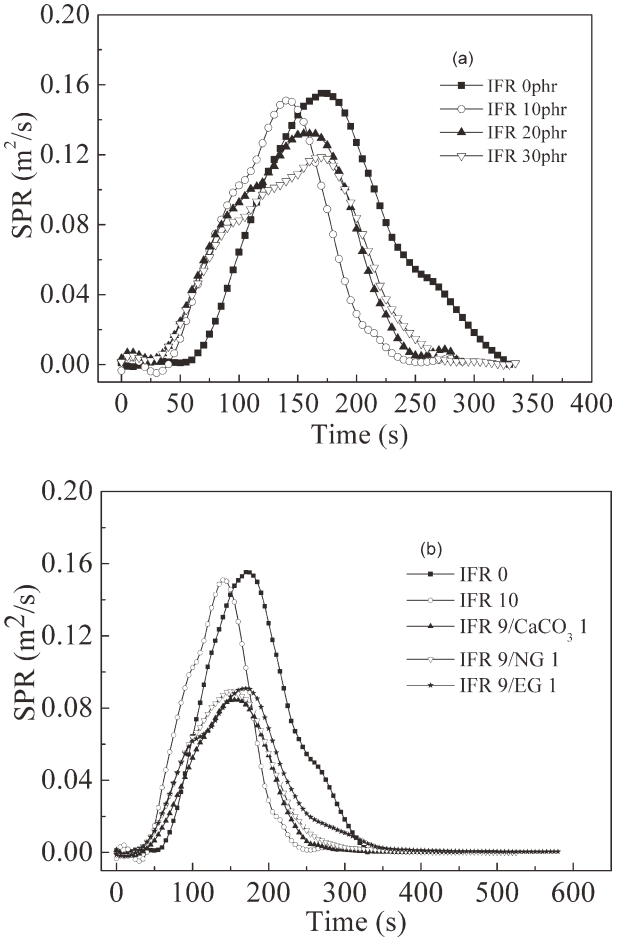

Figure 3 SPR curves versus time for EVA/IFR (APP/PER/ZB) (a) and its optimized composites with $CaCO_3$, NG, and EG (b).

and the morphology was observed by SEM to find the reasons why the char had the function to improve the flame retardant resistance.

Combustion behaviors of EVA/IFR composites and EVA/IFR/synergist composites

Combustion process of EVA/IFR composites

It should be mentioned that char residues for all composites show a typical intumescent morphology. Uniform, intact, and swollen char layers produced in initial period of a fire function as the "barrier" to the materials and hinder the volatilization of combustible gases and retard the penetration of oxygen and feedback of heat flux, and cause a significantly enhancement of flame retardancy. Taken EVA/IFR (10 phr) composite as an example, the dynamic evolution of the combustion progress in cone calorimeter can be described in Figure 5.

From the photos in Figure 5, it can be seen that the sample is gradually intumescent (1, 2) due to the effect of heat radiation and flame at beginning, then ignited (3) at 44s which can be got in Table II and Figure 1, and charring on the surface (4) of the composite to protect the under material in the combustion process. As the accumulation of heat, it can be found that the surface char is gradually destroyed and become smaller gradually because it cannot resist the sustaining heat radiation (5) and some stronger char which will induce the second HRR peak (seen in Fig. 1) may emerge in the surface of the composite. Finally, some gray char residue remains over the aluminum foil for the composite (6).

Residual mass in combustion process

General speaking, the enhancement of fire retardancy of materials is attributed to the barrier effect of carbonaceous char formed in combustion. Char forming performance of intumescent flame retarded composites could also be confirmed by cone test as shown in Figure 6. Figure 6 shows the dynamic curves of residual mass versus combustion time for EVA/IFR (a) and EVA/IFR/Synergist (b) composites. Meanwhile, an amount of residues obtained in

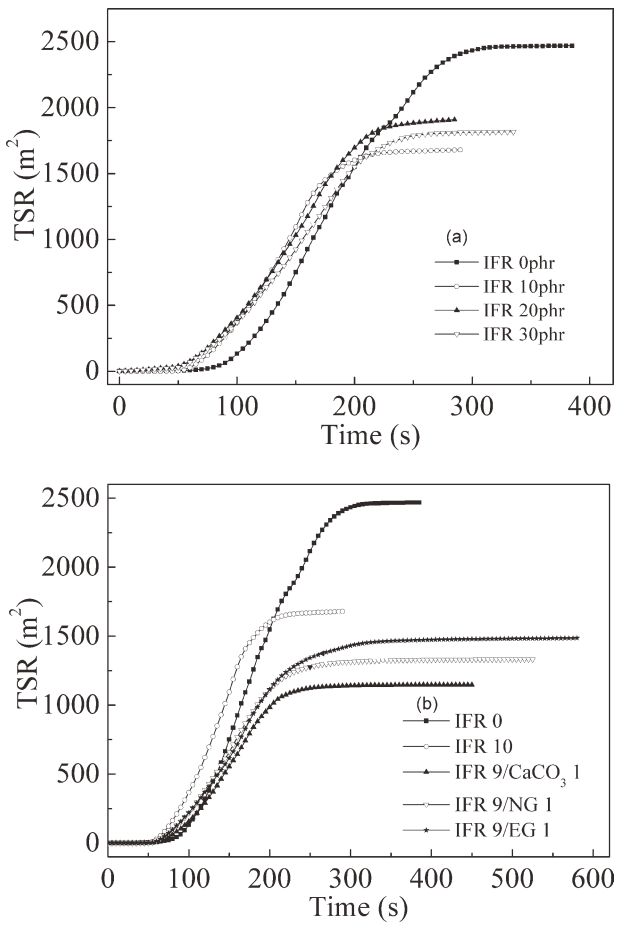

Figure 4 TSR curves versus time for EVA/IFR (APP/PER/ZB) (a) and its optimized composites with $CaCO_3$, NG, and EG (b).

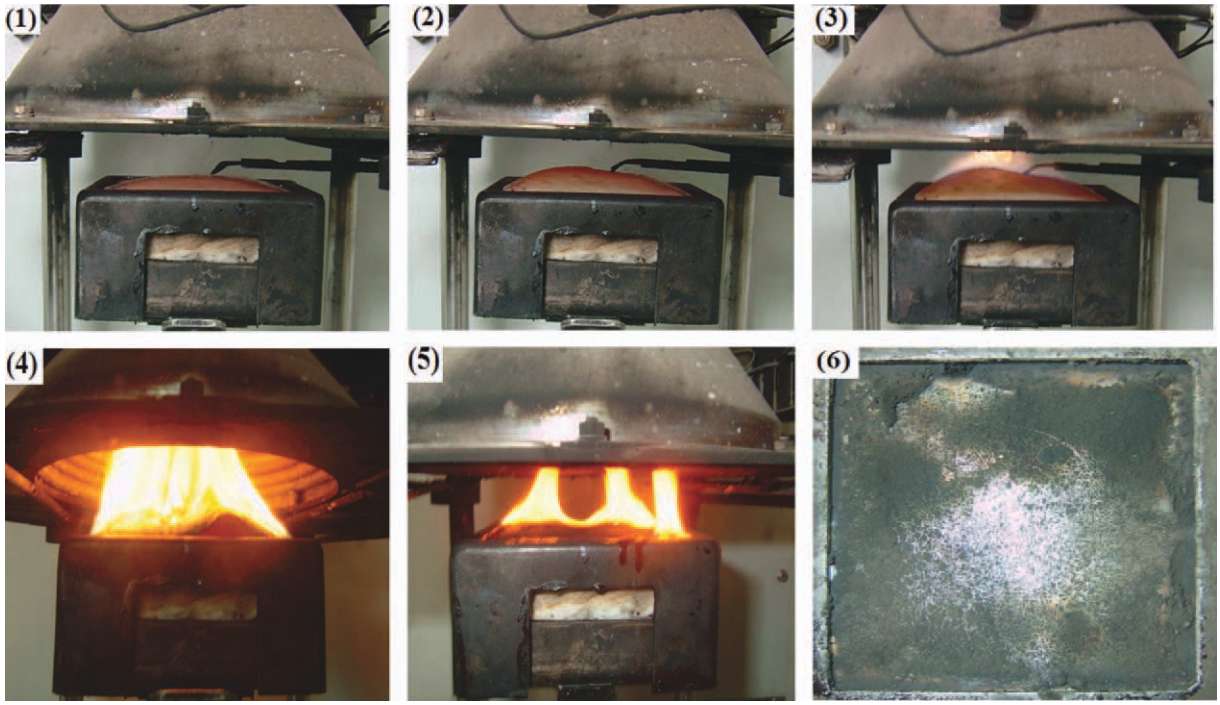

Figure 5 The dynamic evolution of the combustion progress for EVA/IFR (10 phr) in cone calorimeter. [Color figure can be viewed in the online issue, which is available at wileyonlinelibrary.com.]

the cone test confirms the presence of carbonaceous char.

It can be seen that while pure EVA is completely burnt at 300 s, only 1.5% residue (which is almost in the error range) is left. The EVA/IFR (1, 20, and 30 phr) composites still have about 6.8, 10.2, and 11.9% of their original weights due to the high charring capacity of IFR. By the addition of $CaCO_3$, NG, and EG in EVA/IFR composites, the residue weights increase to 8.3, 8.6, and 8.4%, higher than that of EVA/IFR (10 phr; 6.8%), indicating char formation promoting effect of $CaCO_3$, NG, and EG.

The slope of the dynamic curves of residual mass versus combustion time presents the MLR in Figure 6. It can be seen that MLR of EVA/IFR composites is significantly lower than that of pure EVA, the more IFR content the lower of MLR. MLR is recognized to be the primary parameter responsible for decreasing the HRR and SPR of a material during combustion. When adding IFR and synergist, the MLR data also showed that $CaCO_3$, NG, or EG is an effective synergistic agent in EVA/IFR/Synergist system. From the results above, it is shown that both the IFR and the synergist give good flame retardance and smoke suppression.

Intumescent char residues left in combustion process

Considering IFR mainly plays its role in condensed phase by porous carbonaceous char, that is, an increase in char formation is favorable to the reduction of heat release and thus, is an indication of good fire retardant effectiveness. Therefore, it is necessary to investigate the microstructure of char residues to further understand the flame retardant mechanisms.

Figure 7(a–f) shows the residual images of pure EVA, EVA/IFR, and EVA/IFR/Synergist composites after combustion in cone calorimeter. It could be found that the pure EVA had been burnt out and all the aluminum foil became visual, while the others for the flame-retardant EVA composites remained more or less residues and incumbent nearly or completely on the aluminum foil. Seen from Figure 7(a–c), the phenomenon of the more IFR content the more chars on the aluminum foil can be found, indicating that the forming char effect of the IFR in EVA composites on the combustion progress. Compared with the EVA/IFR composites with the same IFR content (10 phr), it could be found that the char residues presented more on the foil evidently for the EVA/IFR/Synergist composites, especially in Figure 7(f) there is cracked and collapsed phenomenon for the char residues because of the dramatic expansion in combustion. Therefore, the synergist has good flame retardant effect on the EVA/IFR/synergist composite even the content of synergist is only 1 phr in the composite, and a significant synergistic IFR effect exists between EG and IFR when applied in EVA matrix. The synergist $CaCO_3$, NG, or EG is not only the char source, but also the gas

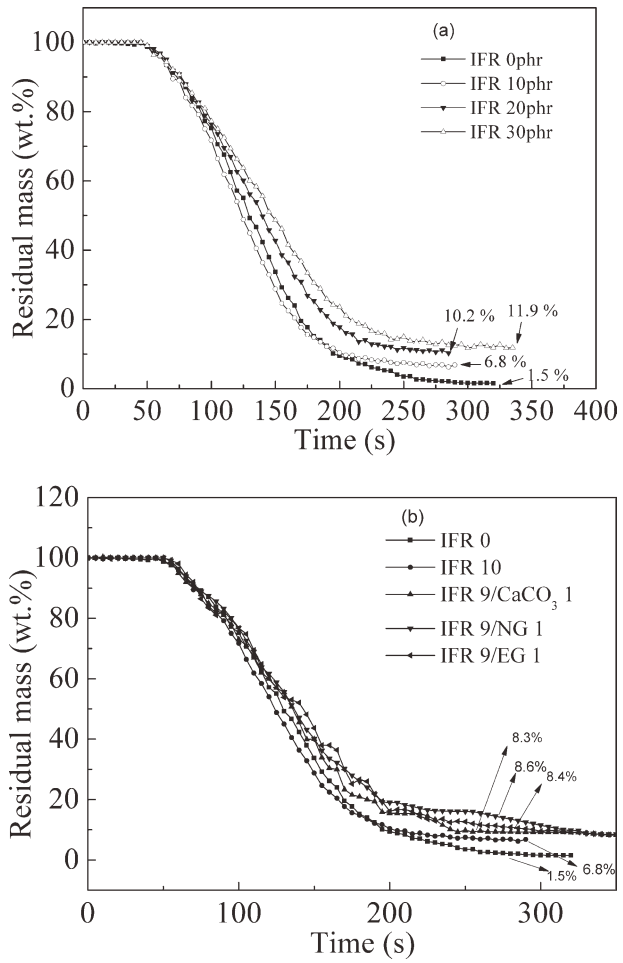

Figure 6 The dynamic curves of residual mass versus combustion time for EVA/IFR (a) and EVA/IFR/Synergist composites (b).

source because of the expansion in the combustion process. The consolidated char layer forms a barrier, which can reduce heat and low molecular transfer and air incursion and thus enhances the flame retardant performance.

Morphology of intumescent char residues from different systems by SEM

Intumescent systems are known to act mainly in the condensed phase via the formation of an insulating barrier. The formation of the effective protective char layer could prevent the heat transfer between the flame zone and the burning substrate, and thus protect the underlying materials from further burning and retard the pyrolysis of polymers during combustion. To further investigate the effect of IFR and Synergists ($CaCO_3$, NG, and EG) on the char formation of flame-retardant EVA composites during combustion, the morphologies of the char residues left after cone calorimetry test were characterized by SEM in Figure 8. In Figure 8, it could be seen that all the samples swell to a certain extent and the charred layer appears in the process of combustion. Char residues for all composites show a typical intumescent morphology.

In Figure 8(a,b), the char residue microstructure of IFR/EVA composites without synergistic agent is so loose, like loose soil just plowed by a tractor, and there are many crevasses and holes on the surface of char residue. Therefore, heat and flammable volatiles could easily penetrate the char layer into the flame zone during the process of burning. Although IFR (APP/PER/ZB system in this paper) takes a role in flame retardant in the IFR/EVA composites, it needs to add high loadings to reach the flame retardant target. So some synergist should be added in the IFR/EVA composites to optimize the flame retardant formula. The char residue surface morphology containing synergist is improved based on Figure 8(a,b), and the microstructure of the char layer seems to be thicker and solider than the former.

The microstructure of char residue containing $CaCO_3$ [Fig. 8(c,d)] is distinctly different from above samples, which char layer microstructure is fine and intertwined each other, like a carpet. It has been proved that decarbonation reaction occurs during burning for the IFR/polymer system.[68] $CaCO_3$ would become to CaO and CO_2, CO_2 could act as a blowing agent to swell to all the directions in the combustion process. It could be seen that the char swells so much bigger and the bulk density was likely smaller than that of other chars in Figure 8, indicating that the char has bigger volume to resist the fire.

In Figure 8(e–h), the chars swell next to the flame and are being expanded in a leaf-like overlapped morphology. These can be explained by the following descriptions. EG is a flake graphite compound intercalated by sulfuric acid between the crystal carbon layers of the nature graphite.[69–74] When exposed to a heat source over 220°C, carbon and sulfuric acid reacts and generates gases that lead to the voluminous expansion of EG more than 100 times of its initial volume in the direction perpendicular to the carbon layers in the crystal structure.[70,74–77] But, NG is a layered material, consisting of a graphene nanosheet structure where carbon atoms are bound by covalent bonds to other carbons in the same plane, while van der Waals interactions keep adjacent layers together.[78–80] The intumescent EG in EVA/IFR/EG composite overlapped each other to form the structure, which seems more compact than that of EVA/IFR/NG composite in the combustion process. From the pictures in Figure 8, it can be imagined that NG and EG with different expansion coefficients because of different environmental temperatures intercrosses and overlaps between the flame and blends. It also can be found

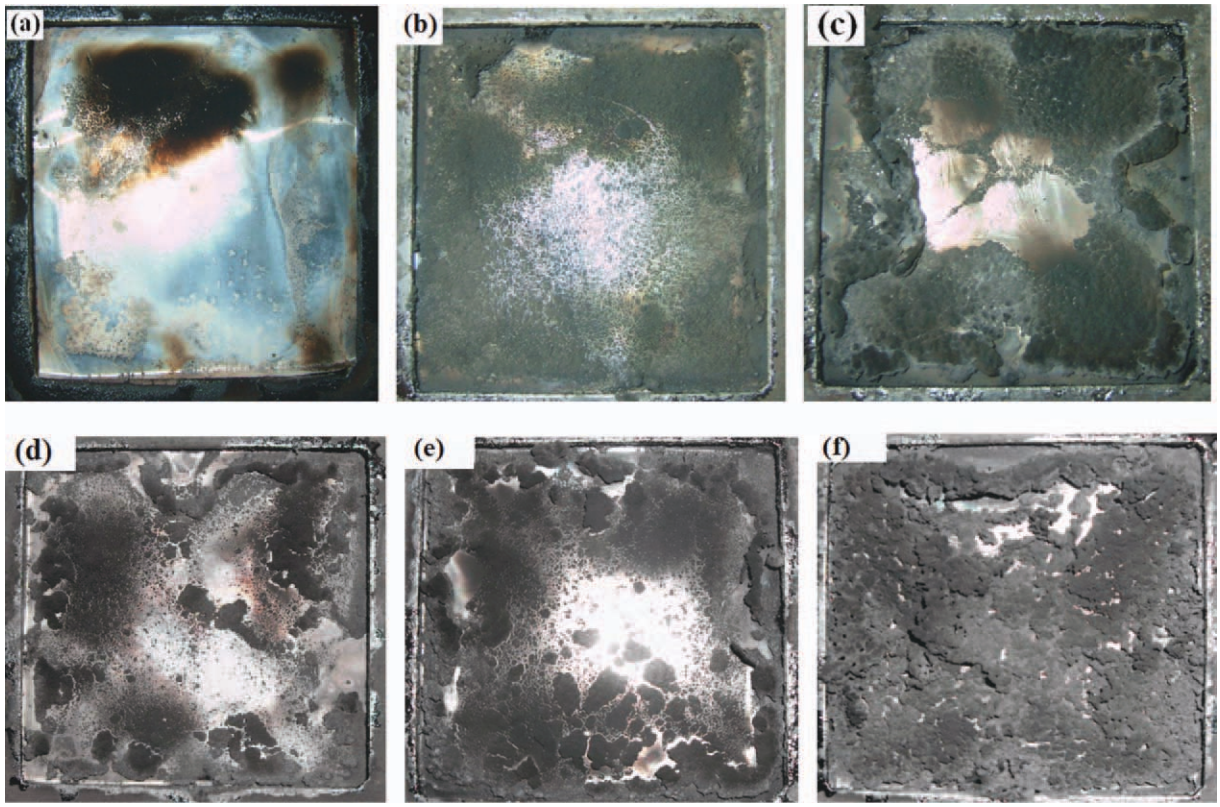

Figure 7 Photographs of residual char for EVA/IFR (APP/PER/ZB) and its optimized composites: (a) pure EVA; (b) IFR 10 phr; (c) IFR 30 phr; (d) IFR 9/$CaCO_3$ 1; (e) IFR 9/NG 1; (f) IFR 9/EG 1. [Color figure can be viewed in the online issue, which is available at wileyonlinelibrary.com.]

that there are many small carbon balls sticking to the surface of NG and EG graphite. The flowing carbon particles would subsequently deposit on the surface of graphite flakes, and consequently generates the folding structure. Once formed it would execute much better heat and oxygen resistance. There are some big hollowsphere (cell structure or alveolate structure, broken, or closed) in the chars of EVA/IFR/NG, which seem that they are easy to fracture, but the carbon balls of the char layer for EVA/IFR/EG composite are all closed. The closed structural carbon balls improve the thermal protection properties of char layer, which is in good agreement with the cone results. These indicate that IFR may have a better synergistic effect with EG than that with NG in EVA composites. Compared with Figure 8(a,b), if the chars of EVA/IFR samples like loose soil, the chars of EVA/IFR /EG samples would like beton arme, showing the good synergistic effect of IFR with EG.

Based on the above analysis, one can conclude that not only char quantity but also char quality formed during combustion are crucial to the flame retardance ability of EVA composites and the incorporation of synergist can generate more compact char and modify the barrier formed in the intumescent flame retarded system so as to achieve a higher degree of fire retardation.

Thermal stabilities of intumescent char residues from different systems by TGA

In the case of IFR polymeric materials, IFRs' could generate a swollen multicellular thermally stable char on heating, which insulated the underlying material from the flame action and resulted in the extinguishment of combustion.[1,81] From above results, we know that not only char quantity but also char quality formed during combustion are crucial to the flame retardance ability of EVA composites. Information on the yield and thermal stability of intumescent char can be obtained through TGA, which provides the possibility to predict the flammability performance for the fire safety researcher. In this section, TGA was used to test thermal stability of intumescent char residues.

Figure 9 shows the TGA curves versus temperature for residues left in the cone calorimeter test of EVA/IFR and its optimized composites. The curve of the char residual of EVA/IFR (10 phr) begins to decrease under 100°C because of the volatilization of

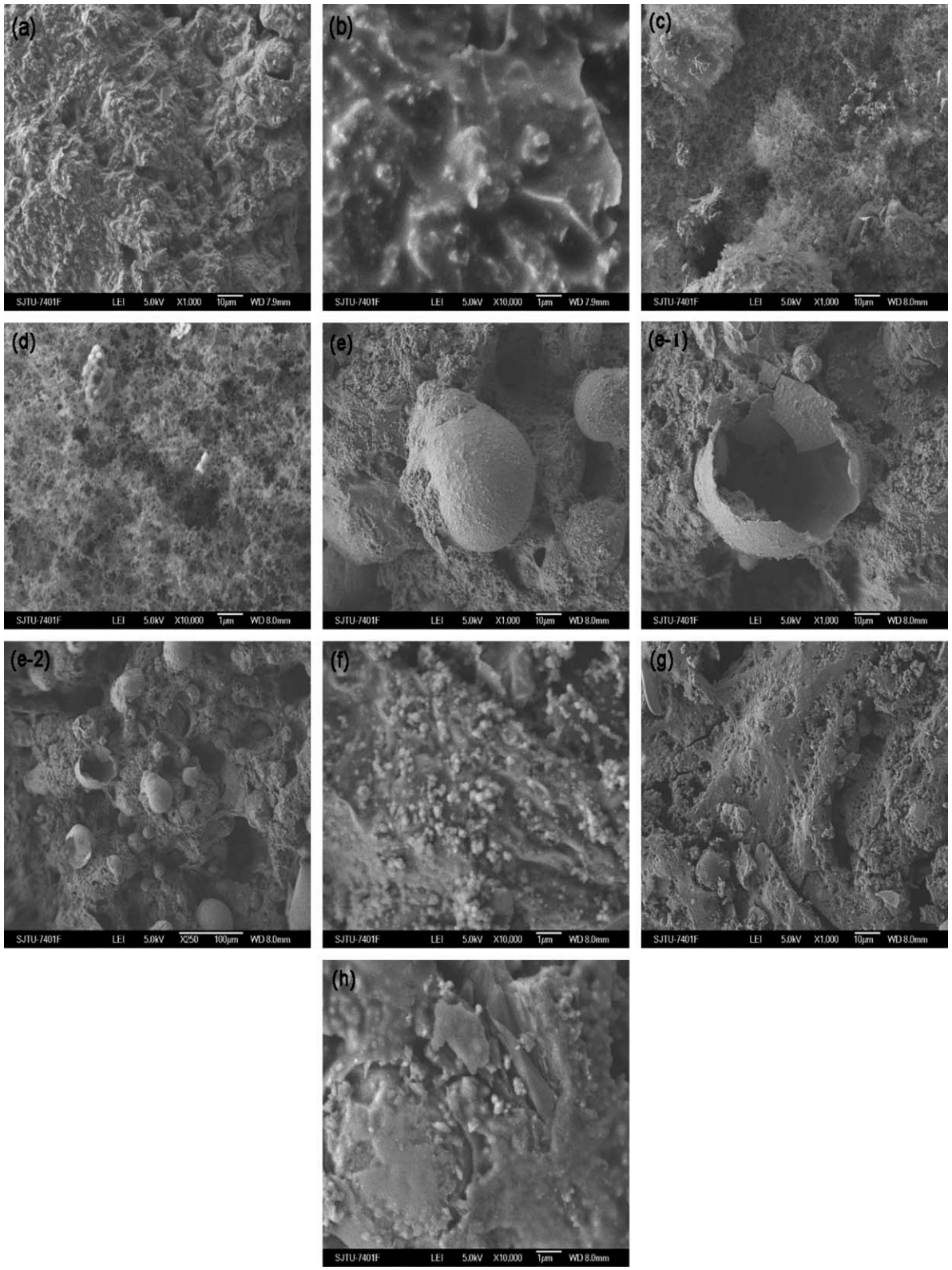

Figure 8 SEM images of residual char for EVA/IFR and its optimized composites after fire in cone calorimeter: (a, b) IFR 10; (c, d) IFR 9/$CaCO_3$ 1; (e, e-1, e-2,f) IFR 9/NG 1; (g, h) IFR 9/EG 1.

some small molecules, and then decreases to 64.7% because of the decomposition of the char residual. The curves of the char residual of EVA/IFR/Synergist almost have no drop before 600°C, and then reduce to 91.2, 73.8, and 72.0%, respectively, which are all higher than 64.7%, indicating that the char layer formed by EVA/IFR/Synergist composites are all more stable than that of the char formed by

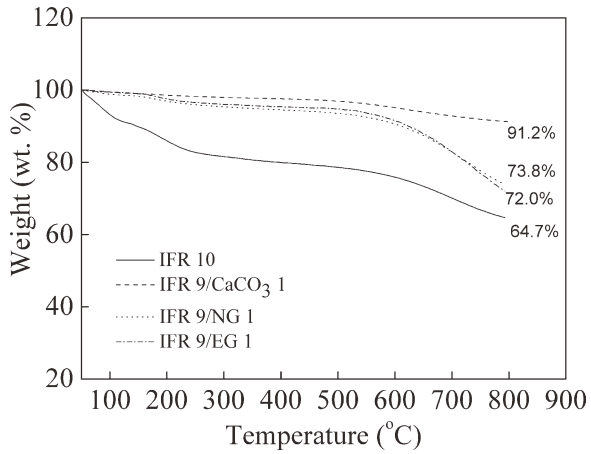

Figure 9 TGA curves versus temperature for residues of EVA/IFR and its optimized composites.

EVA/IFR composite in the combustion process. These data discussed above, which are in agreement with results of the flame retardancy and SEM images of residual char, provide positive evidence that synergists ($CaCO_3$, NG, and EG) could increase the stability of the char residual of the flame retarded EVA composites, and further prove the important of char quality formed during combustion.

CONCLUSIONS

EVA/IFR (APP/PER/ZB system) and EVA/IFR/Synergist ($CaCO_3$, NG, or EG) composites have been prepared by melting compounding method. The results show that HRR, THR, and SPR reduce following the increasing IFR concentration. The data on flammability characterization from the cone calorimeter tests show that the synergist ($CaCO_3$, NG, or EG; 1 phr) combined with IFR additive (9 phr) decreases significantly the HRR, THR, and SPR values of EVA/IFR/Synergist composite. The flame retardant mechanism might be mainly a result of the formation of intumescent charred layers in the condensed phase, which slow down heat and mass transfer between the gas and the condensed phases and limit the diffusion of oxygen to the polymer bulk.

The quantity and the quality of the residual chars of EVA/IFR and EVA/IFR/Synergist are investigated to illustrate the phenomenon above. The EVA/IFR (10, 20, and 30 phr) composites still have about 6.8, 10.2, and 11.9% of their original weights due to the high charring capacity of IFR, while there is almost no residual left for pure EVA. By the addition of $CaCO_3$, NG, EG in EVA/IFR composites, the residue weights increase to 8.3, 8.4, and 8.6%, higher than that of EVA/IFR (10 phr; 6.8%), indicating char formation promoting effect of $CaCO_3$, NG, and EG.

The morphological structure of the residue chars of EVA composites were observed by SEM. The results show that the forming structure (like carpet structure for $CaCO_3$, leaf-like overlapped structure with carbon balls for NG and EG) of the EVA/IFR composites with the synergist are useful to the flame retardance.

The thermal stabilities of intumescent char residues from different systems by TGA also showed that the residual chars reduced to 91.2% ($CaCO_3$), 73.8% (NG), and 72.0% (EG) after 800°C, respectively, which are all higher than 64.7% (only IFR), indicating that the char layer formed by EVA/IFR/Synergist composites are all more stable than that of the char formed by EVA/IFR composite in the combustion process, providing positive evidence that synergists ($CaCO_3$, NG, and EG) could increase the stability of the char residual of the flame retarded EVA composites, and further proving the important of char quality formed during combustion. The quantity and quality of the chars of EVA/IFR/Synergist composite may be the main reasons to enhance the flame retardance and may provide theoretical guidance to scientific research and industry.

References

1. Wang, L. C.; Wu, X. F.; Wu, C.; Yu, J. H.; Wang, G. L.; Jiang, P. K. J Appl Polym Sci 2011, 121, 68.
2. Wu, X. F.; Wang, L. C.; Wu, C.; Yu, J. H.; Xie, L. Y.; Wang, G. L.; Jiang, P. K. Polym Degrad Stab 2012, 97, 54.
3. Li, B.; Jia, H.; Guan, L. M.; Bing, B. C.; Dai, J. F. J Appl Polym Sci 2009, 114, 3626.
4. Le Bras, M.; Bourbigot, S.; Revel, B. J Mater Sci 1999, 34, 5777.
5. Du, L. C.; Qu, B. J.; Xu, Z. J. Polym Degrad Stab 2006, 91, 995.
6. Chacko, A.; Sadiku, E. R.; Vorster, O. C. J Reinforced Plast Compos 2010, 29, 558.
7. Camino, G.; Maffezzoli, A.; Braglia, M.; De Lazzaro, M.; Zammarano, M. Polym Degrad Stab 2001, 74, 457.
8. Cai, Y. B.; Hu, Y.; Song, L.; Lu, H. D.; Chen, Z. Y.; Fan, W. C. Thermochim Acta 2006, 451, 44.
9. Bugajny, M.; Bourbigot, S.; Le Bras, M.; Delobel, R. Polym Int 1999, 48, 264.
10. Basfar, A. A.; Mosnacek, J.; Shukri, T. M.; Bahattab, M. A.; Noireaux, P.; Courdreuse, A. J Appl Polym Sci 2008, 107, 642.
11. Alongi, J.; Poskovic, M.; Frache, A.; Trotta, F. Polym Degrad Stab 2010, 95, 2093.
12. Ye, L.; Qu, B. J. Polym Degrad Stab 2008, 93, 918.
13. Marosfoi, B. B.; Garas, S.; Bodzay, B.; Zubonyai, F.; Marosi, G. Polym Adv Technol 2008, 19, 693.
14. Liu, H.; Fang, Z. P.; Peng, M.; Shen, L.; Wang, Y. C. Radiat Phys Chem 2009, 78, 922.
15. Fernandez, A. I.; Haurie, L.; Formosa, J.; Chimenos, J. M.; Antunes, M.; Velasco, J. I. Polym Degrad Stab 2009, 94, 57.
16. Beyer, G. Fire Mater 2005, 29, 61.
17. Basfar, A. A.; Bae, H. J. J Fire Sci 2010, 28, 161.
18. Xie, F.; Wang, Y. Z.; Yang, B.; Liu, Y. Macromol Mater Eng 2006, 291, 247.
19. Jiao, C. M.; Wang, Z. Z.; Ye, Z.; Hu, Y.; Fan, W. C. J Fire Sci 2006, 24, 47.
20. Hirschler, M. M.; Piansay, T. Fire Mater 2007, 31, 373.
21. Zhang, J.; Hereid, J.; Hagen, M.; Bakirtzis, D.; Delichatsios, M. A.; Fina, A.; Castrovinci, A.; Camino, G.; Samyn, F.; Bourbigot, S. Fire Saf J 2009, 44, 504.

22. Morganl, A. B.; Cogent, J. M.; Opperman, R. S.; Harris, J. D. Fire Mater 2007, 31, 387.
23. Lv, J.; Qiu, L. Z.; Qu, B. J. Nanotechnology 2004, 15, 1576.
24. Beyer, G. Fire Mater 2001, 25, 193.
25. Almeras, X.; Dabrowski, F.; Le Bras, M.; Poutch, F.; Bourbigot, S.; Marosi, G.; Anna, P. Polym Degrad Stab 2002, 77, 305.
26. Almeras, X.; Dabrowski, F.; Le Bras, M.; Delobel, R.; Bourbigot, S.; Marosi, G.; Anna, P. Polym Degrad Stab 2002, 77, 315.
27. Lewin, M. Polym Degrad Stab 2005, 88, 13.
28. Horrocks, A. R.; Kandola, B. K.; Davies, P. J.; Zhang, S.; Padbury, S. A. Polym Degrad Stab 2005, 88, 3.
29. Wang, Z. Y.; Han, E. H.; Ke, W. J Appl Polym Sci 2007, 103, 1681.
30. Morgan, A. B. Polym Adv Technol 2006, 17, 206.
31. Ma, H. Y.; Tong, L. F.; Xu, Z. B.; Fang, Z. P. Appl Clay Sci 2008, 42, 238.
32. Isitman, N. A.; Gunduz, H. O.; Kaynak, C. Polym Degrad Stab 2009, 94, 2241.
33. Du, B. X.; Guo, Z. H.; Song, P. A.; Liu, H.; Fang, Z. P.; Wu, Y. Appl Clay Sci 2009, 45, 178.
34. Beyer, G. Polym Adv Technol 2006, 17, 218.
35. Yang, D. D.; Hu, Y.; Song, L.; Nie, S. B.; He, S. Q.; Cai, Y. B. Polym Degrad Stab 2008, 93, 2014.
36. Lv, P.; Wang, Z.; Hu, Y.; Yu, M. Plast Rubber Compos 2008, 37, 311.
37. Li, G. X.; Yang, J. F.; He, T. S.; Wu, Y. H.; Liang, G. Z. Surf Coat Technol 2008, 202, 3121.
38. Lewin, M.; Endo, M. Polym Adv Technol 2003, 14, 3.
39. Lewin, M. Polym Adv Technol 2001, 12, 215.
40. Vannier, A.; Duquesne, S.; Bourbigot, S.; Castrovinci, A.; Camino, G.; Delobel, R. Polym Degrad Stab 2008, 93, 818.
41. Zanetti, M.; Camino, G.; Thomann, R.; Mullhaupt, R. Polymer 2001, 42, 4501.
42. Marosi, G.; Marton, A.; Anna, P.; Bertalan, G.; Marosfoi, B.; Szep, A. Polym Degrad Stab 2002, 77, 259.
43. Hu, Y.; Wang, S. F.; Ling, Z. H.; Zhuang, Y. L.; Chen, Z. Y.; Fan, W. C. Macromol Mater Eng 2003, 288, 272.
44. Ye, L.; Wu, Q. H.; Qu, B. J. Polym Degrad Stab 2009, 94, 751.
45. Morlat-Therias, S.; Fanton, E.; Gardette, J. L.; Peeterbroeck, S.; Alexandre, M.; Dubois, P. Polym Degrad Stab 2007, 92, 1873.
46. Ma, H. Y.; Tong, L. F.; Xu, Z. B.; Fang, Z. P. Adv Funct Mater 2008, 18, 414.
47. Liu, L.; Wang, Y.; Li, Y. L.; Wu, J.; Zhou, Z. W.; Jiang, C. X. Polymer 2009, 50, 3072.
48. Zhang, M.; Ding, P.; Du, L. C.; Qu, B. J. Mater Chem Phys 2008, 109, 206.
49. Zhang, G.; Ding, P.; Zhang, M.; Qu, B. Polym Degrad Stab 2007, 92, 1715.
50. Wu, Q.; Qu, B. J. Polym Degrad Stab 2001, 74, 255.
51. Nyambo, C.; Kandare, E.; Wilkie, C. A. Polym Degrad Stab 2009, 94, 513.
52. Li, Y. T.; Li, B.; Dai, J. F.; Jia, H.; Gao, S. L. Polym Degrad Stab 2008, 93, 9.
53. Du, B. X.; Guo, Z. H.; Fang, Z. P. Polym Degrad Stab 2009, 94, 1979.
54. Chen, X. L.; Jiao, C. M. Fire Saf J 2009, 44, 1010.
55. Song, R. J.; Zhang, B. Y.; Huang, B. T.; Tang, T. J Appl Polym Sci 2006, 102, 5988.
56. Li, J. M.; Wilkie, C. A. Polym Degrad Stab 1997, 57, 293.
57. Wang, L. C.; Wang, G. L.; Jiang, P. K. J Appl Polym Sci 2011, 120, 368.
58. Nazare, S.; Kandola, B. K.; Horrocks, A. R. Polym Adv Technol 2006, 17, 294.
59. McNally, T.; Potschke, P.; Halley, P.; Murphy, M.; Martin, D.; Bell, S. E. J.; Brennan, G. P.; Bein, D.; Lemoine, P.; Quinn, J. P. Polymer 2005, 46, 8222.
60. Beyer, G. J Fire Sci 2005, 23, 75.
61. Schartel, B.; Bartholmai, M.; Knoll, U. Polym Adv Technol 2006, 17, 772.
62. Marney, D. C. O.; Russell, L. J.; Mann, R. Fire Mater 2008, 32, 357.
63. Carpenter, K.; Janssens, M. Fire Technol 2005, 41, 79.
64. Ren, W. T.; Peng, Z. L.; Zhang, Y.; Zhang, Y. X. J Appl Polym Sci 2004, 92, 1804.
65. Bourbigot, S.; LeBras, M.; Delobel, R.; Breant, P.; Tremillon, J. M. Polym Degrad Stab 1996, 54, 275.
66. Jiao, C. M.; Chen, X. L. Polym Eng Sci 2010, 50, 767.
67. Peng, H. Q.; Zhou, Q.; Wang, D. Y.; Chen, L.; Wang, Y. Z. J Ind Eng Chem 2008, 14, 589.
68. Bellayer, S.; Tavard, E.; Duquesne, S.; Piechaczyk, A.; Bourbigot, S. Polym Degrad Stab 2009, 94, 797.
69. Cuesta, J. M. L.; Swoboda, B.; Buonomo, S.; Leroy, E. Polym Degrad Stab 2008, 93, 910.
70. Duquesne, S.; Le Bras, M.; Bourbigot, S.; Delobel, R.; Vezin, H.; Camino, G.; Eling, B.; Lindsay, C.; Roels, T. Fire Mater 2003, 27, 103.
71. Li, Z. M.; Bian, X. C.; Tang, J. H.; Lu, Z. Y.; Lu, A. J Appl Polym Sci 2007, 104, 3347.
72. Morgan, A. B.; Higginbotham, A. L.; Lomeda, J. R.; Tour, J. M. ACS Appl Mater Interfaces 2009, 1, 2256.
73. Singha, N. K.; Thirumal, M.; Khastgir, D.; Manjunath, B. S.; Naik, Y. P. J Appl Polym Sci 2008, 110, 2586.
74. Wang, Z. Y.; Han, E.; Ke, W. Corros Sci 2007, 49, 2237.
75. Duquesne, S.; Delobel, R.; Le Bras, M.; Camino, G. Polym Degrad Stab 2002, 77, 333.
76. Schartel, B.; Braun, U.; Schwarz, U.; Reinemann, S. Polymer 2003, 44, 6241.
77. Webster, D. C.; Chattopadhyay, D. K. Prog Polym Sci 2009, 34, 1068.
78. Chen, C. Y.; Wang, G. A.; Cheng, W. M.; Tu, Y. L.; Wang, C. C. Polym Degrad Stab 2006, 91, 3344.
79. Hu, G. H.; Pan, Y. X.; Yu, Z. Z.; Ou, Y. C. J Polym Sci Part B: Polym Phys 2000; 38, 1626.
80. Wang, J. A.; Zhang, P.; Song, L.; Lu, H. D.; Hu, Y. A. Energy Conversion Manage 2010, 51, 2733.
81. Kandola, B. K.; Horrocks, A. R.; Horrocks, S. Fire Mater 2001, 25, 153.